Improving the Corrosion Behaviour of 6061 Aluminum Alloy by Controlled Anodic Formed Oxide Layer

VALENTIN MARIAN DUMITRASCU, LIDIA BENEA*
Dunarea de Jos University of Galati, Research (Competence) Center: Interfaces-Tribocorrosion and Electrochemical Systems (CC-ITES), Faculty of Engineering, 47 Domnească Str., 800008, Galați, România

This research work investigates the influence of anodic oxide film obtained in sulphuric electrolyte on the corrosion behavior of 6061 aluminum alloy in natural sea water. Corrosion behavior of untreated and anodized 6061 aluminum alloy was studied using electrochemical methods such as: open circuit potential and electrochemical impedance spectroscopy. All the tests were performed in an aerate sea water with pH=7.63 at room temperature (25°C). The electrochemical results are in good agreement with optical microscopy images. The polarization resistance of aluminum oxide film increases as compared with the untreated aluminum alloy this showing an improving of corrosion resistance after anodic oxidation. These results demonstrate the advantages of the as-fabricated anodic oxide layer as a barrier thin film to marine corrosion.

Keywords: Aluminum alloy, anodic oxidation, corrosion, electrochemical impedance spectroscopy

New developments in the transport industry, especially in marine and aeronautical fields are intimately related to the development and use of materials which are stronger, lighter, more corrosion resistant and more temperature resistant. It is well known that aluminum and its alloys have a huge number of applications due to excellent comprehensive physical and chemical properties. These properties can be attributed to a rapidly formed surface oxide film (Al_2O_3, $Al(OH)_3$, $AlO(OH)$), at air exposure, with 3-7 nm thickness.

However, the thin oxide layer is not sufficient to protect against corrosion agents such as chlorides ions, sulfate ions, etc. Aggressive ions can be absorbed into the faults and voids and their penetration and accumulation lead to oxide layer destruction [1, 2].

The aluminum alloys remain the subject of numerous studies due to their susceptibility to localized corrosion attack in more aggressive environments [3]. Especially in chloride environment, peak-aged aluminum alloys tend to show increased susceptibility to pitting corrosion and stress corrosion cracking [3-6]. So, it is in high demand to develop highly effective and selective method to counter this phenomenon.

Actually, many studies have been carried out and different protective methods have been reported [1]. Corrosion is usually prevented by chemical passivation coatings [7, 8], polymer coatings [9] and anodized coatings [10].

Aluminum and its alloys are highly reactive materials and to improve their durability in many environments they are often subjected to anodizing and sealing processes [11].

Anodic films, composed, in specially, of amorphous alumina, are formed by application of an anodic potential to aluminum sheet which is immersed in a suitable electrolytes. When are used slightly alkaline electrolytes or close to neutrality due to lowest solubility of the oxide, a compact oxides (barrier-type layer) are usually generated [12]. In contrast, when the solubility of the oxide is increased, porous oxide layers can be formed [10].

The anodic oxide film characteristics formed on the aluminum surface and the intensity of corrosion attack are influenced by (a) chemical composition of the alloy, (b) the presence of the micro or macro–defects and also (c) the chemical composition of the electrolyte. The pitting corrosion occurs when the pH is ranged between 4.5–8.5 and tends to increase with an increase of temperature, concentration of aggressive ions and stagnation of the electrolyte [4].

Chloride ions from marine environment can alter the corrosion behavior of aluminum alloy due to the distribution of the intermetallic phases and localized corrosion, pitting corrosion as well as intergranular corrosion, etc. can occur.

The aims of this research work are to study and compare the corrosion behavior of untreated and anodized 6061 aluminum alloy (AA 6061) by electrochemical methods in natural sea water harvest from Black Sea, Mangalia port.

Experimental part
Materials and methods
For the experimental part it was used 6061 aluminum alloy provided from Color Metal SRL (Bucharest, Romania) with chemical composition presented in table 1.

Before the anodization process, two sets of samples were prepared. Rectangular plates with dimensions 20x20x2 mm were connected with copper wire and isolated with epoxy resin to delimit the active surface. The samples were degreased with acetone, rinsed with

Element	Si	Fe	Cu	Mn	Mg	Cr	Zn	Ti	Al
Composition (wt %)	0.4	0.2	0.15	0.15	0.8	0.04	0.25	0.15	Balance

Table 1
CHEMICAL COMPOSITION OF 6061 ALUMINUM ALLOY (% BY WEIGHT)

*email: Lidia Benea@ugal.ro

deionized water and dried at room temperature.

In the electrochemical cell for anodization process the used anode was an AA 6061 sample, described above, and as cathode it was used an AA 6061 plate with an active surface of 5 cm². The anodizing process was carried out at room temperature (25±1°C) applying a constant current density of 45 mA/cm² in 300 mL of 1 M sulfuric acid (H_2SO_4) solution to which 1 g/L of aluminum sulfate octadecahydrate ($Al_2(SO_4)_3$ 18H_2O) was added.

After the anodization process, the samples were washed with deionized water and the pores were sealed for 5 minutes at 95°C in boiling water.

The corrosion behavior of untreated AA 6061 and anodized AA 6061 samples was studied in natural sea water from Black Sea, Mangalia harbour. The sea water has the following characteristics: pH=7.63, electrical conductivity=21 mS/cm and salinity=12.4 ‰.

The electrochemical cell used for corrosion tests contained Platinum-Rhodium (Pt-Rh) grid as counter electrode, untreated or anodized AA 6061 sample as working electrode and an Silver/Silver Chloride/Potassium Chloride saturated solution (Ag/AgCl/KCl) with E=199 mV vs. standard hydrogen electrode (SHE) as reference electrode. The surface area of sample exposed to the corrosive solution was delimited at 1.79 cm². The electrochemical tests were done using a Potentiostat/ Galvanostat VoltaLab PGZ 100 and data were recorded with VoltaMaster software, version 4.0.

The applied electrochemical methods were the open circuit potential (OCP) – time plots and electrochemical impedance spectroscopy (EIS).

The open circuit potential (OCP) measurements were monitored during the exposure time of 60 min until has been reached the steady state potential vs. Ag/AgCl reference electrode. The electrochemical impedance spectroscopy was carried out at open circuit potential after the potential was stabilized. Frequency of a.c. voltage excitation signal ranged from 100 kHz to 10 mHz, with 20 points per decade recording, using 10 mV peak-to-peak sinusoidal potential amplitude. The impedance spectra were fitted using the ZView 3.4e software.

The surface morphology of untreated and anodized 6061 aluminum alloy, before and after electrochemical assays was evidenced using the optical microscope OPTIKA XDS-3 MET. The optical images were performed with software Vision Pro Plus, version 5.0 on computer connected to optical microscope.

Results and discussions
Optical microscopy before and after surface treatment

Before and after the anodic oxidation process, the sample surface was subjected to optical microscopy investigation, in order to observe the surface modifications which appeared after the surface treatment was applied.

Figure 1 presents the surface morphology of untreated and anodic oxidated AA 6061. From figure 1a it can be observed that the surface of untreated AA6061 is characterized by irregularly shape, scratches and defects due to polish process. The anodized and sealed sample presented a rough surface with homogenous distribution (fig. 1b). After the boiling in deionized water the pores of barrier oxide layer were sealed. The anodic film generated on 6061 aluminum alloy presented relatively straight pores and continuous cell walls. This occurs because the simultaneous oxidation of the major alloying element, magnesium, with aluminum and does not induce oxygen generation within the barrier layer and consequent lateral porosity [13].

Open circuit potential – time curves

In figure 2 it is shown the variation in time of the open circuit potential of untreated and anodized 6061 aluminum alloy as function of time in natural sea water after immersion for one hour (fig. 2a) and 9.5 h (fig. 2b).

From figure 2a it is observed that the OCP of untreated AA6061 sample fluctuates around -670 mV vs. Ag/AgCl due to the dissolution of native passive film in presence of chloride ions. The OCP of anodized 6061 aluminum alloy increases in the first 5 min after immersion in natural sea water and after that it decreases under the action of chloride ions reaching a steady state potential around value of -425 mV vs. Ag/AgCl.

After 9.5 h of immersion (fig. 2b), the open circuit potential of untreated AA6061 sample retains the same fluctuation trend with mean value of potential around -675 mV vs. Ag/AgCl. The OCP value of anodized AA 6061 decreases slowly after 9.5 h of immersion, from -425 mV to -440 mV vs. Ag/AgCl.

Moreover, comparing the potential values of untreated and anodized aluminum alloy surfaces, it is clearly revealed that the surface treatment improves the corrosion resistance through shifting the potential to a more noble
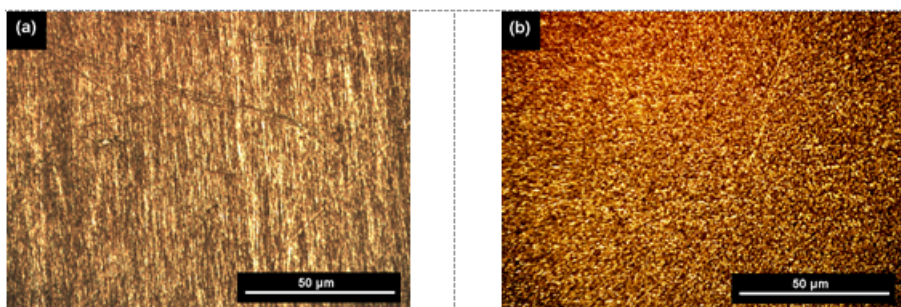

Fig. 1. Optical microscopy of: (a) Untreated AA6061 surface and (b) Anodized AA6061 surface
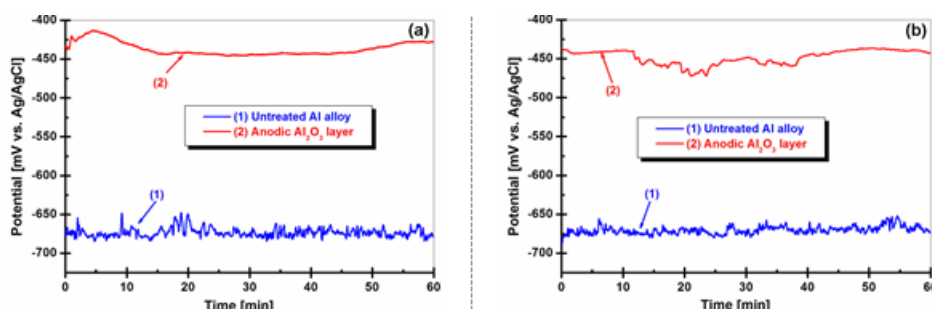

Fig.2. Open circuit potential after immersion of (1) untreated 6061 aluminum alloy and (2) anodized 6061 aluminum alloy in natural sea water (a) for 1 h and (b) for 9.5 h
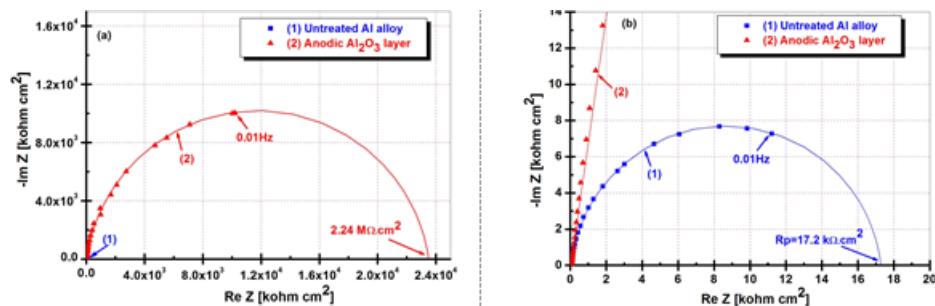
Fig. 3. Nyquist representation of EIS data for: (■) untreated and (▲) anodized 6061 aluminum alloy. (a) Experimental data and fitted diagrams (b) zoom of Nyquist representation to show the diagram of untreated Al alloy. The plain symbol corresponds to the experimental data and the solid line correspond to fitted diagram
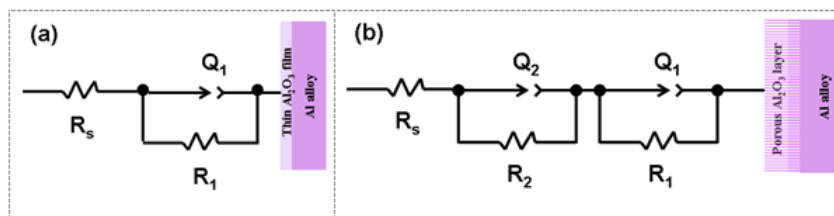

Fig. 4. Equivalent circuit for fitting the experimental EIS data of: (a) untreated 6061 aluminum alloy and (b) anodic oxidation 6061 aluminum alloy

value. The potential shift to nobler (positive) direction is often associated with the formation of a protective passive film at the alloy surface [5]. This trend was also observed by L. Benea et al [14] for controlled anodic oxide layer on Ti-6Al-4V alloy.

Electrochemical impedance spectroscopy

Nyquist plots of the electrochemical impedance spectroscopy measurements (experimental data and their fitted response) of untreated and anodized 6061 aluminum alloy, recorded in unstirred natural sea water are presented in figure 3a. The specific resistance of untreated aluminum alloy is very small comparatively with those of anodized surface therefore it was necessary to present in figure 3b a zoom of diagrams from figure 3a, to show the experimental and fitted data for untreated alloy.

In order to estimate the appropriate equivalent electrical circuit, a deep understanding of the system is necessary. Electrochemical cell may be represented by an equivalent circuit (CE), consisting from different resistors combinations, capacitors and other circuit elements [15]. For untreated aluminum alloy it can be considered a solid electrode (aluminum alloy) in contact with natural sea water having a very thin and inhomogeneous oxide layer instantaneously formed in air. The equivalent circuit is given in figure 4a. By anodizing process on the aluminum surface it is formed a homogenous aluminum oxide layer, which by boiling in deionized water becomes very protective, as it is proposed in the equivalent circuit from figure 4b.

In figure 4a and 4b, Rs is the solution resistance, R_1 is the ohmic resistance and Q_1 is the constant phase element of native oxide layer, respectively. In figure 4b, R_2 and Q_2 are the ohmic resistance and the constant phase element of anodized oxide layer.

Simple elements such as resistances, capacitances, inductances or convective diffusion can't often reveal the impedance results of solid electrode/electrolyte interface which is frequency dispersion. The frequency dispersion is generally attributed to a *capacitance dispersion* expressed in terms of a constant-phase element (CPE). The time

constant dispersion was attributed to a dispersion of the capacity or to a change of the capacity with frequency and its expression was proposed by Brug et al. [16] as:

$$Z_{CPE} = \frac{Q}{(j\omega)^{1-\alpha}} \quad (1)$$

where:

$j = \sqrt{-1}$, ω is the angular frequency ($\omega=2\pi f$, f being the frequency in Hz), Q is a frequency-independent real constant of the CPE ($\Omega \cdot cm^2 \, s^{-(1-\alpha)}$) and $(1-\alpha)$ is related to the angle of rotation of a purely capacitive line on the complex plane plots.

Depending on the formula used, the CPE parameter is Q, $1/Q$ or Q^a for capacitance dispersion and is used to represent a circuit parameter with limiting behaviour as a capacitor for $\alpha=1$, a resistor for $\alpha=0$ and an inductor for $\alpha=-1$.

Also, different origins and expressions of the CPE have been discussed in the literature [17, 18]. In our corrosion experiments we could consider the origins of CPE behaviour as being the surface heterogeneities and electrode porosity.

The specific polarization resistance (R_p) is an indicative of the kinetics of the charge transfer reactions or rate of dissolution [19] and was obtained following the fitting of the impedance experimental results by using the equivalent circuits proposed in figure 4a and 4b [14, 18].

The diameter of the semicircle decides the corrosion resistance of the coatings, and a larger diameter means the higher the corrosion resistance [11]. Polarization resistance (R_p) increases from 17.2 *kohm cm²* corresponding to untreated 6061 aluminum alloy to 2.24 *Mohm cm²* for anodized 6061 aluminum alloy. Thus, the increase in the polarization resistance leads to an increasing of corrosion resistance of anodized aluminum alloy.

Optical microscopy analysis after corrosion

In figure 5a and 5b are presented the optical microscopy images after 9.5 h of electrochemical assays. It can be observe that the surface morphology of untreated AA 6061
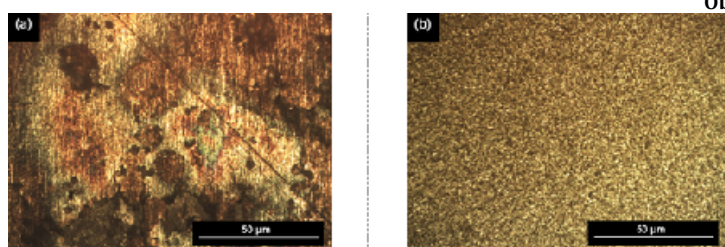

Fig. 5. Optical microscopy after corrosion assays in natural sea water of (a) untreated AA6061 and (b) anodized AA6061

(fig. 5a) is affected by aggressive ions from natural sea water during the corrosion tests while the anodized AA 6061 (fig. 5b) is not seriously affected.

Comparing the figure 1a of untreated AA6061 before corrosion test with figure 5a after 9.5 h of corrosion tests in natural sea water, it can be observed large corroded areas with irregular shapes and variable depths. Also, on the untreated surface numerous pits with irregular distribution are presented.

Similarly, by comparing the figure 1b of oxidized AA6061 alloy before corrosion tests with figure 5b after 9.5 h of corrosion tests in natural sea water, it can be seen that the oxidized aluminum surface did not suffer any corrosion attack. This confirms that the anodic formed aluminum oxide layer protects very well the aluminum alloy surface against corrosive marine environment.

Conclusions

The aluminum oxide layer was successfully formed on AA6061 alloy surface and the corrosion resistances of untreated and anodized 6061 aluminum alloy were comparatively studied by electrochemical and optical methods. It was found that the open circuit potential of oxidized aluminum alloy is more noble compared with that of untreated alloy during immersion time in marine corrosive environment.

Electrochemical impedance spectroscopy is an ideal method to characterize the electrolyte-metal interface and to quantify the changes of the barrier layer during immersion time. The Nyquist diagrams show that the polarization resistance of 6061 aluminum alloy after anodic treatment increases with about two orders of magnitude from 17.2 $kohm\ cm^2$ to 2.24 $Mohm\ cm^2$. The electrochemical results are in good agreement with the optical microscopy images.

References

1. ALLACHI, H., CHAOUKET, F., DRAOUI, K., J. Alloys Compd., **491**, 2010, p. 223.
2. ROSLIZA, R., SENIN, H.B., WAN NIK, V.B., Colloid Surface A, **312**, 2012, p. 185.
3. TRUEBA, M., TRASATTI, S.P., Mater. Chem. Phys., **121**, 2010, p.523.
4. EZUBER. H., EL-HOUD, A., EL-SHAWESH, F., Mater. Design, **29**, 2008, p. 801.
5. ZAID, B., SAIDI, D., BENZAID, A., HADJI, S., Corros. Sci., **50**, 2008, p. 1841.
6. DONUTS, U., THOMPSON, G.E., ELABAR, D., HASHIMOTO, T., MORSCH, S., Surf. Coat. Tech., **277**, 2015, p. 91.
7. RAJ, V., MUBARAK ALI, M., J. Mater. Process. Technol., **209**, 2009, p. 5341.
8. KIYOTA, S., VALDEZ, B., STOYTCHEVA, M., ZLATEV, R., BASTIDAS, J.M., J. Rare Earths, **29**, no. 10, 2011, p. 691.
9. ZUBILLAGA, O., CANO, F.J., AZKARATE, I., MOLCHAN, I.S., THOMPSON, G.E., SKELDON, P., Thin Solid Films, **517**, 2009, p. 6742.
10. FELIU, Jr.S., BARTOLOME, M.J., GONZALEZ, J.A., LOPEZ, V., FELIU, S., Appl. Surf. Sci., **254**, 2008 p. 2755.
11. FELIU, Jr.S., GONZALEZ, J.A., LOPEZ, V., BARTOLOME, M.J., ESCUDERO, E., OTERO, E., J. Appl. Electrochem., **37**, 2005 p.1027.
12. CHANG, J.K., LIAO, C.M, CHEN, C.H, TSAI W.T., J. Electrochem. Soc., **150**, no. 6, 2003, p. B266.
13. GARCIA-RUBIO, M., OCON, P., CURIONI, M., THOMPSON, G.E., SKELDON, P., Corros. Sci., **52**, 2010, p. 2219.
14. BENEA, L., MARDARE-DANAILA, E., MARDARE, M., CELIS, J.P., Corros. Sci., **80**, 2014, p. 331.
15. BRUG, G.J., VAN DEN EEDEN, A.L.G., SLUYTERS-REHBACH, M., SLUYTERS, J.H., J. Electroanal. Chem., **176**, 1984, p. 275.
16. SOLTANI, N., TAVAKKOLI, N., KHAYATKASHANI, M., JALALI, M.R., MOSAVIZADE, A., Corros. Sci., **62**, 2012, p. 122.
17. HUANG, V.M.W., VIVIER, V., FRATEUR, I., ORAZEM, M.E., TRIBOLLET, B., J. Electrochem. Soc., **152**, 2007, p. C89
18. CIUBOTARIU, A.C., BENEA, L., LAKATOS-VARSANYI, M., DRAGAN, V., Electrochim. Acta., **53**, 2008, p. 4557